Seham H. Salman
Noor Alhuda Hassan
Ghuzlan S. Ahmed
Hanaa I. Mohammed
Shaimaa A. Abbas

Department of Physics, College of Education for Pure Sciences / Ibn Alhaitham, University of Baghdad, Baghdad, IRAQ

Effect of Annealing Time on Physical Properties of TiO_2 Thin Films Prepared by RF Magnetron Sputtering Technique

The rf magnetron sputtering technique was utilized to prepare titanium dioxide (TiO_2) thin films on glass substrates. These films were annealed for one hour at temperatures of 400, 500 and 600°C. The UV-visible-NIR spectrophotometry was used to characterize the prepared films in order to determine their optical constants. The Field-emission scanning electron microscopy (FE-SEM) was used to determine the film thickness. The results showed that the transmittance of these films increases as the annealing temperature is increased. In the visible region of spectrum, the index of refraction of the prepared films was ranging from 2.22 to 1.2. The extinction coefficient was very low in the visible region and it increased with increasing annealing temperature. The gas sensitivity of TiO_2 films increase in the temperature range of 200-1400°C even at low NO_2 concentrations. The film annealed at 600°C shows high sensitivity to NO_2 gas at ambient temperature and this sensitivity increases at operation temperature of 100°C.

Keywords: Reactive sputtering; Surface morphology; Annealing temperature; Optical properties
Received: 11 August 2023; **Revised:** 02 October 2023; **Accepted:** 09 October 2023

1. Introduction

Recently, a lot of research has been done on titanium dioxide (TiO_2) because of its interesting optical properties. Wide band gap TiO_2 films are employed in a range of applications including the optics industry, due to their high refractive index [1-4]. The highly transparent in visible and infrared spectral range, have been widely used as antireflection coatings for increasing the visible transmittance in heat mirrors [5,6]. It is one of the frequently utilized materials for antireflection coatings [7] and photocatalysts [8-12]. Due to its excellent stability at higher temperatures, TiO_2 is utilized to detect a variety of gases. Since the use detectors is very important for preventing the hydrogen leak, the necessity for hydrogen detecting equipment becomes crucial [13]. Three crystalline phases are anatase (tetragonal), rutile (tetragonal), and brookite (orthorhombic) of TiO_2 that can also exist as an amorphous layer. Only rutile phase is thermodynamically stable at high temperature [14,15]. Spray pyrolysis [16], Ion-beam aided deposition [17], Sputtering using a dc reactive magnetron [2,4,18], and rf reactive magnetron sputtering are some of the techniques used [19], sol-gel dip coating technique [20], chemical vapor deposition [21], and plasma enhanced chemical vapor deposition [22] sputter deposition techniques are widely utilized methods to obtain uniform and dense TiO_2 thin films with well-controlled stoichiometry. Heat-treatment is one of the utilized ways to obtain better optical properties of TiO_2 films [23-26].

This study examined the impact of annealing on the structural, optical, and gas sensing characteristics of TiO_2 thin films that were created via Sputtering of RF reactive magnetrons on glass substrates.

2. Experimental Part

Titanium dioxide (TiO_2) thin films were prepared by (RF) magnetron sputtering system with a titanium dioxide target of 99.99% purity on glass slides as substrates. In an ultrasonic bath with acetone and ethanol, the glass slides were cleaned. Before being placed within the vacuum system, they were dried and cleaned with distilled water. As a sputtering target, the disk of the dioxide of titanium (TiO_2) measuring 5 cm in diameter and 3 mm in thickness was employed. As the sputtering and reactive gas, high-purity argon was utilized. Then TiO_2 film deposition at a steady 100-Watt dc power. The deposit time was set to three hours. The sputtering chamber was evacuated 3×10^{-5} Torr, and the working pressure was kept at about 2.5×10^{-3} Torr. The sputtering chamber was evacuated 3×10^{-5} Torr, and the working pressure was kept at about $2.5\text{x}10^{-3}$ Torr. The substrates coated with TiO_2 at room temperature were heated in an electric furnace to 400, 500, and 600°C for one hour to anneal thin films. The UV-visible optical transmission spectra of TiO_2 thin films were measured using UV-visible 1800 spectrophotometer in the wavelength range 300-1100 nm. The films'

optical constants, absorption coefficient, and optical band gap were determined. The optical method (reflectivity) was used to measure film thickness. By using the field-emission electron scanning microscopy (FE-SEM), the thickness of the films as they were being deposited on the cold substrate was double-checked. Thin films for NO_2 gas were used to measure the resistance vs. time at room temperature and temperature at 100°C for gas sensing characteristics.

3. Results and Discussion

Figure (1) displays the cross-section illustration of the TiO_2 film in its as-grown state. It displays film thickness and cross-sectional morphology. It is discovered that the film has a thickness of around 315 nm. In this investigation, the thickness by optical method (reflectance) of the deposited film is determined to be 300 nm, which is consistent with the SEM cross-sectional image.

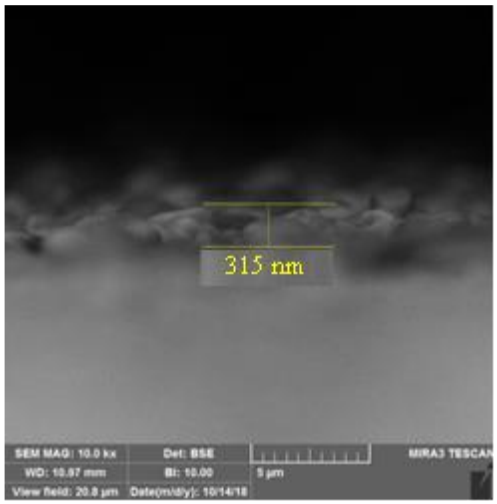

Fig. (1) FE-SEM cross-sectional image of as-deposited film

Table (1) Optical properties of thin films at different annealing temperatures at photon energy of 2.25 eV and wavelength of 550 nm

Sample	α (m^{-1}) 10^2	k	n	ε_r	ε_i	d (s^{-1})
as-deposit	0.834	0.036	2.223	4.942	0.162	4.429
400°C	0.988	0.043	2.655	7.050	0.229	6.270
500°C	0.587	0.025	2.011	4.043	0.103	2.824
600°C	0.069	0.003	1.260	1.588	0.007	2.100

According to Fig. (2), annealing temperature has a negligibly small effect on the crystallinity. FE-SEM images showed that all the films had a homogeneous distribution, very smooth and crystallinity is very good. No large particles can be found in these images, as the particle size ranges in 20-50 nm. Figure (2) shows that the nanostructure contains a certain type of particles and there are also voids that occur between the particles.

The energy-dispersive spectrometry (EDS) was used to ensure that the weight and atomic ratios of the films were correct, and the results are shown in Fig. (3) and the attached table (3).

Table (3) The EDS examination data

Element	Apparent Concentration	Wt.%	Atomic %
O	3.87	54.14	77.95
Ti	4.21	45.86	22.05
Total:		100.00	100.00

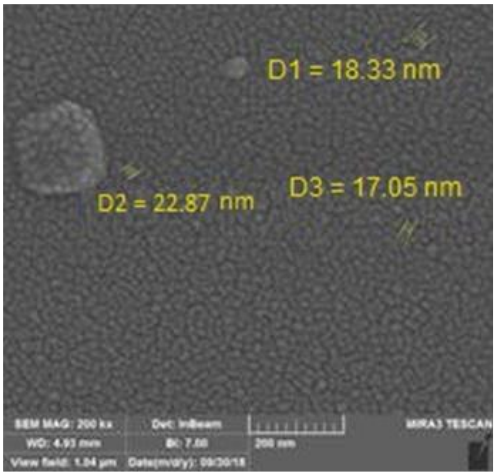

(a)

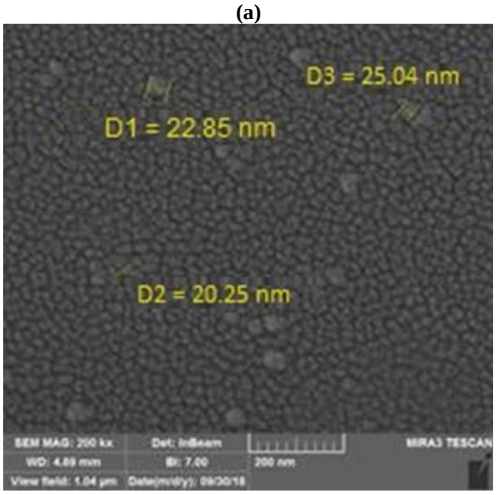

(b)

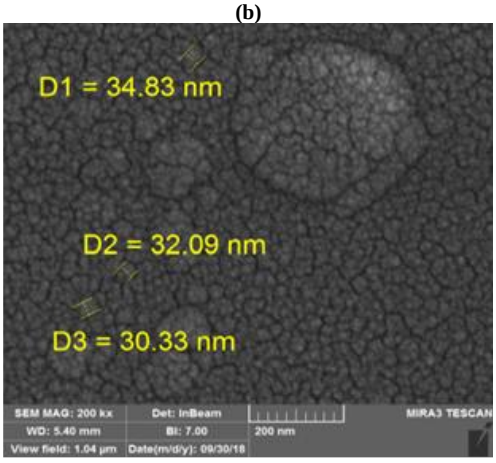

(c)

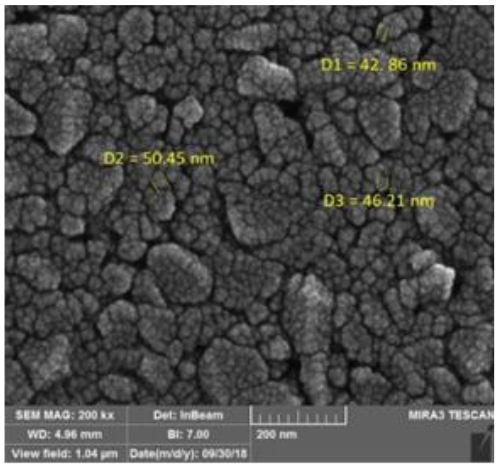

(d)

Fig. (2) The FE-SEM images for TiO_2 and annealed in different temp. Images a (before annealing), b, c and d are for TiO_2 annealed

Figure (4) shows the transmittance of as-deposited and annealed films. They exhibit transmittance between 75 and 95% in the visible and NIR regions. As the annealing temperature is increased, transmittance slightly decreases. Visible light transmittance significantly drops in the films after 600°C annealing. Its enhanced surface roughness may be due to the light scattering effect.

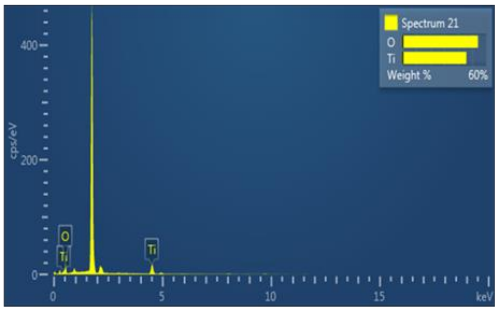

Fig. (3) EDS examination of film deposited on glass

The following equation [27] was used to calculate the absorption coefficient (α):

$$\alpha = 2.303A/t \quad (1)$$

where A stands for absorbance. If the electronic transition is direct or indirect, depending on the optical absorption coefficient (α) of thin films, the optical absorption coefficient ($\alpha>10^4$) is crucial to determining the type of transition.

The relationship between the coefficient of extinction and the absorption coefficient is [28]

$$k = \frac{\alpha\lambda}{4\pi} \quad (2)$$

The optical properties of the films are provided by the refraction index n value, which is determined by the equation below [28].

$$n = \frac{(1+R^{(1/2)})}{(1-R^{(1/2)})} \quad (3)$$

Using the following relationship, the reflectance, R, was calculated: [28]

$$R + T + A = 1 \quad (4)$$

Figure (7) depicts an increase in refractive index both before and after annealing.

Equations (4) and (5) may be used to represent the real (ε_r) and imaginary (ε_i) components of the dielectric constant, respectively [28]:

$$\varepsilon_r = n^2 - k^2 \quad (5)$$

Because they are connected by previous relationship (2), the coefficient of extinction (k) behaves similarly to the coefficient of absorption (α). Figure (5) shows that when the absorption coefficient increases, the values of the extinction coefficient also rise.

$$\varepsilon_i = 2nk \quad (6)$$

Figures (8) and (9) demonstrate the real and imaginary portions of a sample's dependency on photon energy. According to equation (4), ε_r is greater than ε since it is mostly determined by n_2, and the extinction coefficient impact is very minor and may be ignored. Because of the extremely low value of the index refraction [19], the imaginary component is depending on the coefficient of extinction using Eq. (5). The real and imaginary parts in figures (8) and (9) demonstrate that after annealing, there is an increase. This shows that the samples do not have the same structure.

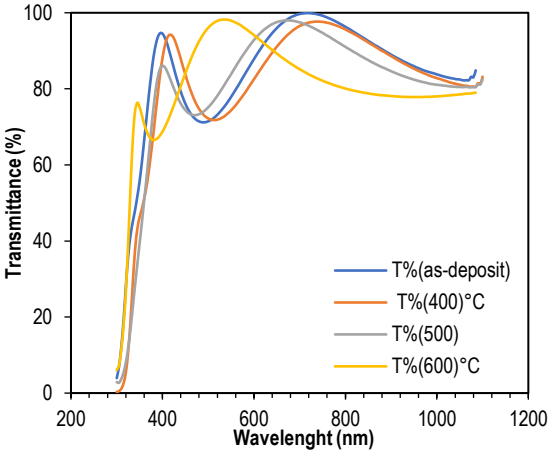

Fig. (4) Demonstrates the relationship between transmittance and the wavelength

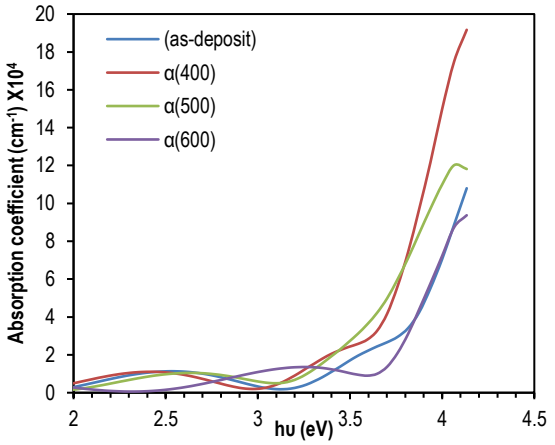

Fig. (5) The relation between absorption coefficient (α) with the (hυ)

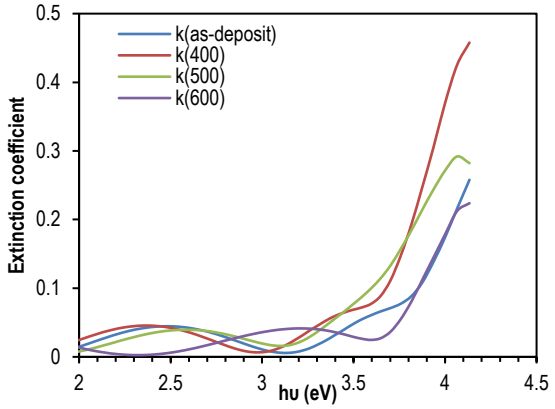

Fig. (6) TiO_2 film extinction coefficient: as-deposited at room temperature, then 400, 500, and 600 °C for annealing

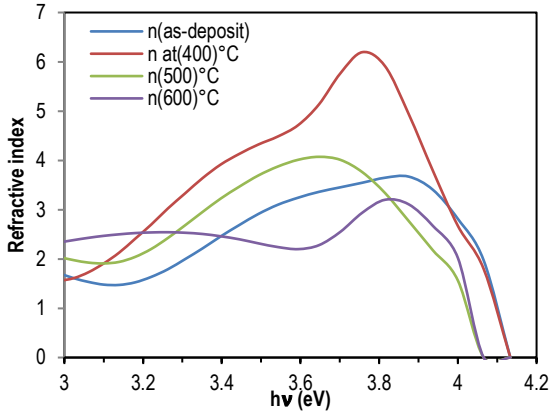

Fig. (7) Depicts the relationship between photon energy and refractive index

Figure (10) demonstrates the relationship between photon energy and optical conductivity. High photon energy causes a rise in optical conductivity, which is followed by a reduction at lower photon energies, because of its dependence on it in accordance with equation, its behavior is similar to that of the absorption coefficient [28]:

$$d = \frac{\alpha n c}{4\pi} \quad (7)$$

The Tauc Model works well in the high absorbance area of the transmittance spectra [29] therefore it is used to estimate the optical band gap of films.

$$\alpha h\nu = b(h\nu - E_g)^r \quad (8)$$

If E_g is the gap of the optical band, b is a constant independent of photon energy, and r has four numerical values (1/2) for allowed direct optical transitions, two for permitted indirect optical transitions, and three for forbidden direct optical transitions, and 3/2 in the case of forbidden indirect optical transitions). This work obtained the direct band gap utilizing $(h\nu)^2$ vs. $h\nu$ curves, which entails the growth of the linear area to low energies. The curves used to evaluate the allowed direct band gap are displayed in Fig. (11), where the decrease of direct band gap with the increase of annealing temperature is also observable. It was reported that for as-deposited and annealed TiO_2 films. The values of energy gap are listed in table (2).

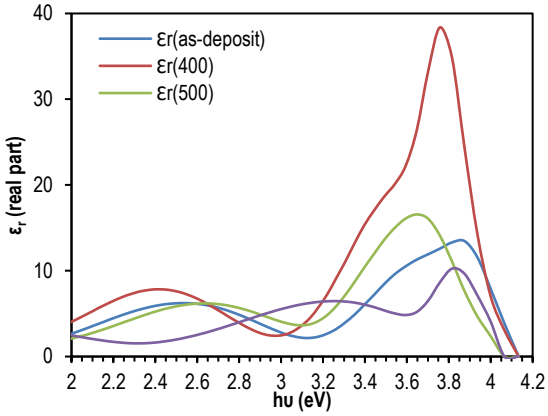

Fig. (8) Depicts the relationship between the real part of the dielectric constant (ε_r) with photon energy

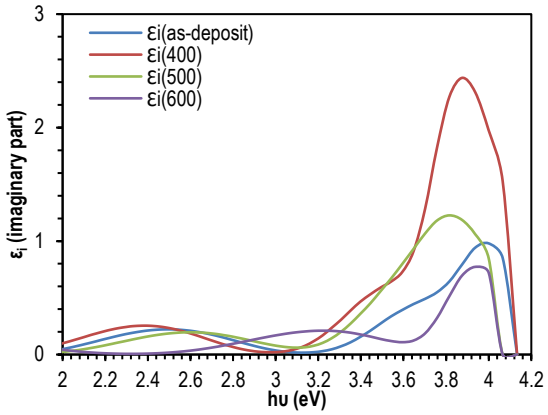

Fig. (9) Depicts the relationship between the imaginary part of the dielectric constant (εi) and energy of the photon

Table (2) Energy gap of thin films for different annealing temperature

Annealing Temperature	E_g (eV)
As-deposit	3.9
400	3.8
500	3.7
600	3.85

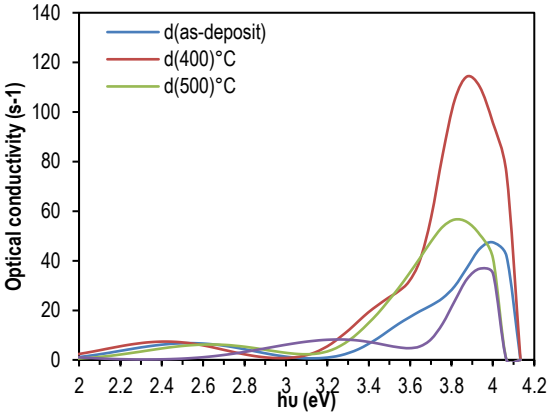

Fig. (10) The relationship between optical conductivity and the energy of the photon

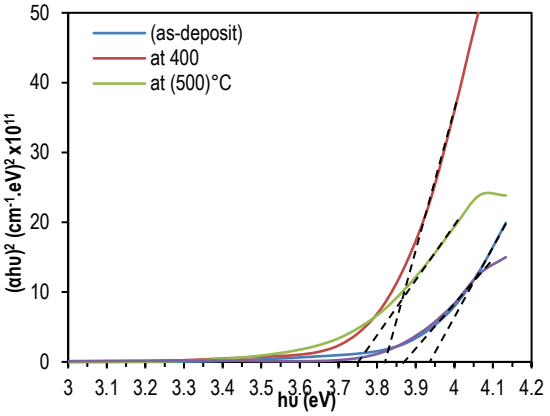

Fig. (11) The relationship between $(\alpha h\nu)^2$ and the curves of energy of TiO_2 films: annealed and deposited and at 400°C, 500°C and 600°C

Because TiO_2 is an n-type semiconductor in general, when an oxidizing gas, such as NO_2, is put into the chamber, the resistance increases from R air to R gas. The sensing characteristics of TiO_2 thin films were investigated, and numerous dynamic responses were recorded as a change in the resistance of the thin film for each sensor. Equation (8) calculates the sensitivity of an n-type semiconductor in the presence of an oxidizing gas [30]

$$S = \frac{\Delta R}{R_g} = \left|\frac{R_g - R_a}{R_g}\right| \times 100\% \qquad (9)$$

Figure (12) shows the typical change of sensitivity for the sample annealed at 600°C and figure (13) sensitivity at operating temperature T_{op} = 100°C. The maximum sensitivity against NO_2 gas appeared at 600°C annealing temperature at 100°C operating temperature is 35.27%.

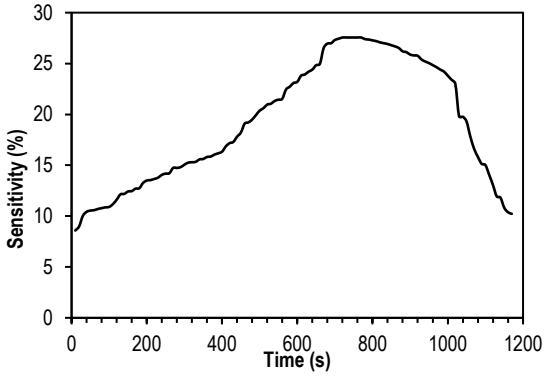

Fig. (12) Sensitivity variation for TiO_2 thin films annealed at 600 °C with NO_2 gas

4. Conclusion

The titanium dioxide thin films were created on unheated glass substrates using RF reactive sputtering. In the visible spectrum, TiO_2 films are very transparent, and annealing treatment produces a modest drop in visual transmittance. The film that is annealed at 600°C has the lowest transmittance. The refractive index at 550 nm wavelength rises in as-grown and annealed TiO_2 films. The energy gap ranged between 3.9 (as-deposited) to 3.85 at 600°C annealing temperature and the obtained results looks far from the standards values lies between 3.0 and 3.2 and we found in the literature that there are other researchers obtained also higher values of energy gap. As the temperature increasing, the extinction coefficient rises. It has been discovered that the permissible direct band gap is decreasing. The film annealed at 600°C has sensitivity for NO_2 gas at ambient temperature and increases sensitivity when measured at 100 °C and the sensitivity is raised from ~28% (at room temperature) to ~70% (at 600°C annealing temperature).

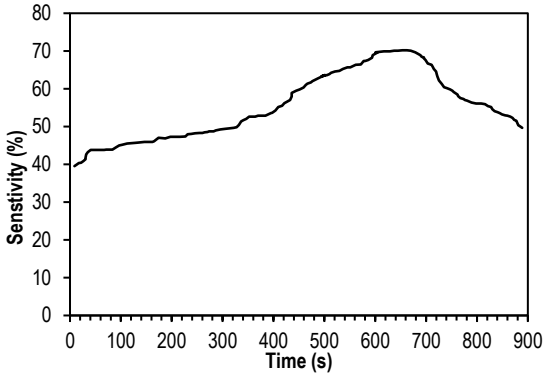

Fig. (13) Sensitivity variation for thin films of TiO_2 annealed at 600°C with operating temperatures 100°C with NO_2 gas

References

[1] T. Ogawa et al., "Enhanced Photocatalytic Activity of TiO_2 Thin Film Deposited by Reactive RF Sputtering under Oxygen-Rich Conditions", *Photochem.*, 2(1) (2022) 138-149.

[2] E.A. Al-Oubidy and F.J. Al-Maliki, "Effect of Gas Mixing Ratio on Energy Band Gap of Mixed-Phase Titanium Dioxide Nanostructures Prepared by Reactive Magnetron Sputtering Technique", *Iraqi J. Appl. Phys.*, 14(4) (2018) 19-23.

[3] M.A. Hameed, S.H. Faisal, R.H. Turki, "Characterization of Multilayer Highly-Pure Metal Oxide Structures Prepared by DC Reactive Magnetron Sputtering Technique", *Iraqi J. Appl. Phys.*, 16(4) (2020) 25-30

[4] A.M. Hameed and M.A. Hameed, "Highly-Pure Nanostructured Metal Oxide Multilayer Structure Prepared by DC Reactive Magnetron Sputtering Technique", *Iraqi J. Appl. Phys.*, 18(4) (2022) 9-14.

[5] M. Okada et al., "Fabrication of photocatalytic heat-mirror with TiO_2/TiN/ TiO_2 stacked layers", *Vacuum*, 80(7) (2006) 732-735.

[6] A.M. Hameed and M.A. Hameed, "Spectroscopic characteristics of highly pure metal oxide nanostructures prepared by DC reactive magnetron sputtering technique", *Emerg. Mater.*, 6 (2022) 627-633.

[7] H. Kawasaki et al., "TiO_2/TiN/TiO_2 heat mirrors by laser ablation of single TiN target", *IOP J. Phys.: Conf. Ser.*, 100(1) (2008) 012038.

[8] O.A. Hammadi, F.J. Kadhim and E.A. Al-Oubidy, "Photocatalytic Activity of Nitrogen-

Doped Titanium Dioxide Nanostructures Synthesized by DC Reactive Magnetron Sputtering Technique", *Nonl. Opt. Quantum Opt.*, 51(1-2) (2019) 67-78.
[9] E.A. Al-Oubidy and F.J. Al-Maliki, "Photocatalytic activity of anatase titanium dioxide nanostructures prepared by reactive magnetron sputtering technique", *Opt. Quantum Electron.*, 51(1-2) (2019) 23.
[10] F.J. Al-Maliki, O.A. Hammadi, B.T. Chiad and E.A. Al-Oubidy, "Enhanced photocatalytic activity of Ag-doped TiO_2 nanoparticles synthesized by DC Reactive Magnetron Co-Sputtering Technique", *Opt. Quantum Electron.*, 52 (2020) 188.
[11] F.J. Kadhim, O.A. Hammadi and N.H. Mutesher, "Photocatalytic activity of TiO_2/SiO_2 nanocomposites synthesized by reactive magnetron sputtering technique", *J. Nanophot.*, 16(2) (2022) 026005.
[12] Z.H. Zaidan, Q.H. Mahmood and O.A. Hammadi, "Using Banana Peels for Green Synthesis of Mixed-Phase Titanium Dioxide Nanopowders", *Iraqi J. Appl. Phys.*, 18(4) (2022) 27-30.
[13] A.A.Haidry et al., "Effect of post-deposition annealing treatment on the structural, optical and gas sensing properties of TiO_2 thin films", *Key Eng. Mater.*, 510 (2012) 467-474.
[14] S.H. Faisal and M.A. Hameed, "Heterojunction Solar Cell Based on Highly-Pure Nanopowders Prepared by DC Reactive Magnetron Sputtering", *Iraqi J. Appl. Phys.*, 16(3) (2020) 27-32.
[15] Z.H. Zaidan, O.A. Hammadi and K.H. Mahmood, "Effect of Structural Phase on Photocatalytic Activity of Titanium Dioxide Nanoparticles", *Iraqi J. Appl. Phys.*, 19(3A) (2023) 55-58.
[16] Q. Ye et al., "Hydrophilic properties of nanoTiO_2 thin films deposited by RF magnetron sputtering", *Vacuum*, 81(5) (2007) 627-631.
[17] I.A. Abbas, S.Q. Hazaa and S.H. Salman, "Employment of Titanium dioxide thin film on NO_2 gas sensing" *IOP J. Phys.: Conf. Ser.*, 1879 (2021) 032061.
[18] C. Yang et al., "Effects of depositing temperatures on structure and optical properties of TiO_2 film deposited by ion beam assisted electron beam evaporation", *Appl. Surf. Sci.*, 254(5) (2008) 2685-2689.
[19] C.J. Tavares et al., "Reactive sputtering deposition of photocatalytic TiO_2 thin films on glass substrates", *Mater. Sci. Eng. B*, 138(2) (2007) 139-143.
[20] S.H. Salman, A.A. Shihab and A.-H.Kh. Elttayef, "Studying The Effect of The Type of Substrate on The Structural, Morphology and Optical Properties of TiO_2 Thin film prepared by Reactive sputtering deposition", *Ener. Proced.*, 157 (2019) 199-207.
[21] A.S Bakri et al., "Effect of Annealing Temperature of Titanium Dioxide Thin Films on Structural and Electrical Properties", *AIP Conf. Proc.*, 1788(1) (2017) 030030-1-8.
[22] H. Sun et al., "Photocatalytic TiO_2 films prepared by chemical vapor deposition at atmosphere pressure", *J. Non-Cryst. Solids*, 354(12-13) (2008) 1440-1443.
[23] W. Yang and C.A. Wolden, "Plasma-enhanced chemical vapor deposition of TiO_2 thin films for dielectric applications", *Thin Solid Films*, 515(4) (2006) 1708-1713.
[24] Y.Q. Hou et al., "Influence of annealing temperature on the properties of titanium oxide thin film", *Appl. Surf. Sci.*, 218(1-4) (2003) 98-106.
[25] O.A. Hammadi, "Effects of Extraction Parameters on Particle Size of Titanium Dioxide Nanopowders Prepared by Physical Vapor Deposition Technique", *Plasmonics*, 15(6) (2020) 1747-1754.
[26] M.K. Ali and F.J. Kadhim, "Structural Characteristics of TiO_2/TiN Nanocomposites Synthesized by DC Reactive Magnetron Sputtering Technique", *Iraqi J. Appl. Phys.*, 19(3A) (2023) 49-54.
[27] F. Scholz, **"Compound Semiconductors"**, McGrow-Hill (1969).
[28] M.G. Yousif, **"Solid State Physics"**, Part 1, University of Baghdad Book House (1989).
[29] J.I. Pankove, "**Optical Processes in Semiconductors**", Dover Publ., Inc. (NY, 1975), Ch. 4, p. 91.
[30] J. Tauc, **"Amorphous and Liquid Semiconductors"**, Plenum Press (London, 1974).

